Simultaneous DNA amplification and detection using a pH-sensing semiconductor system

Christofer Toumazou[1,2], Leila M Shepherd[1], Samuel C Reed[1], Ginny I Chen[1], Alpesh Patel[1,3], David M Garner[1,3], Chan-Ju A Wang[1,3], Chung-Pei Ou[1], Krishna Amin-Desai[1], Panteleimon Athanasiou[1], Hua Bai[1], Ines M Q Brizido[1], Benjamin Caldwell[1], Daniel Coomber-Alford[1], Pantelis Georgiou[2], Karen S Jordan[1], John C Joyce[1], Maurizio La Mura[1], Daniel Morley[1], Sreekala Sathyavruthan[1], Sara Temelso[1], Risha E Thomas[1] & Linglan Zhang[1]

We developed an integrated chip for real-time amplification and detection of nucleic acid using pH-sensing complementary metal-oxide semiconductor (CMOS) technology. Here we show an amplification-coupled detection method for directly measuring released hydrogen ions during nucleotide incorporation rather than relying on indirect measurements such as fluorescent dyes. This is a label-free, non-optical, real-time method for detecting and quantifying target sequences by monitoring pH signatures of native amplification chemistries. The chip has ion-sensitive field effect transistor (ISFET) sensors, temperature sensors, resistive heating, signal processing and control circuitry all integrated to create a full system-on-chip platform. We evaluated the platform using two amplification strategies: PCR and isothermal amplification. Using this platform, we genotyped and discriminated unique single-nucleotide polymorphism (SNP) variants of the cytochrome P450 family from crude human saliva. We anticipate this semiconductor technology will enable the creation of devices for cost-effective, portable and scalable real-time nucleic acid analysis.

Real-time amplification and detection of nucleic acid has fundamentally transformed life science research and molecular diagnostics[1–4]. It has become the standard for rapid detection and quantification of small amounts of nucleic acid and has a wide array of applications. Current technologies for real-time amplification and detection of nucleic acid require devices such as thermal blocks for amplification and precision optics for detection as well as fluorescently labeled sequence-specific probes or fluorescent dyes for labeling DNA[1–4]. In this work, we eliminated the need for all of the above and developed a semiconductor-based amplification device that has thermal actuation integrated with the reaction chemistries and pH-sensing technology, and has the capability to amplify and detect nucleic acid under dynamic pH changes across a broad range of pH[5,6].

The detection platform we chose was the ISFET, a pH-sensing device that is often used to measure ion concentrations in solution[7–11]. ISFETs have previously been used to detect nucleotide incorporation in primer extension assays and have also been proposed as a platform for sequencing[5,12–14]. Based on this concept, Ion Torrent Systems recently developed a semiconductor-based *de novo* nucleic acid sequencer that uses the pH-sensing capability of ISFETs[15]. However, none of these platforms can perform amplification reactions and require off-chip amplification before on-chip analysis.

We leveraged the versatility of standard CMOS design and fabrication to create an integrated circuit, which can amplify and simultaneously detect DNA using embedded heaters, temperature sensors and ISFET sensor arrays. We thereby eliminate the need for bulky external peripheral apparatuses. Unlike the fabrication of previously reported chip technologies for DNA analysis where post-processing such as deposition of gold[16,17] or tantalum pentoxide[15] is required, the fabrication of our chip uses the unmodified CMOS process flow found in standard computer microchip technology, thus making this a low-cost and disposable thermocycling platform.

We created a fingernail-sized semiconductor integrated circuit powered and controlled by a battery-operated microelectronic reader. We illustrate the speed and performance of the integrated circuit by performing real-time amplification and pH-mediated detection using two methods: PCR and loop-mediated isothermal amplification (LAMP)[18]. The platform can genotype DNA from saliva samples in 30 min, which signifies its capability to integrate DNA chemistry and consumer microchip technology.

RESULTS

pH amplification reaction

Our method detects the change in pH as the nucleic acid polymerization reaction proceeds and converts the chemical signals (H^+) into electrical signals using ISFETs as pH sensors[11] (**Supplementary Note 1**). Binding of the complementary primer

[1]DNA Electronics Ltd., London, UK. [2]Department of Electrical and Electronic Engineering, Imperial College London, South Kensington Campus, London, UK. [3]These authors contributed equally to this work. Correspondence should be addressed to C.T. (chris.toumazou@dnae.co.uk) or L.M.S. (leila.shepherd@gmail.com).

RECEIVED 26 NOVEMBER 2012; ACCEPTED 8 MAY 2013; PUBLISHED ONLINE 9 JUNE 2013; DOI:10.1038/NMETH.2520

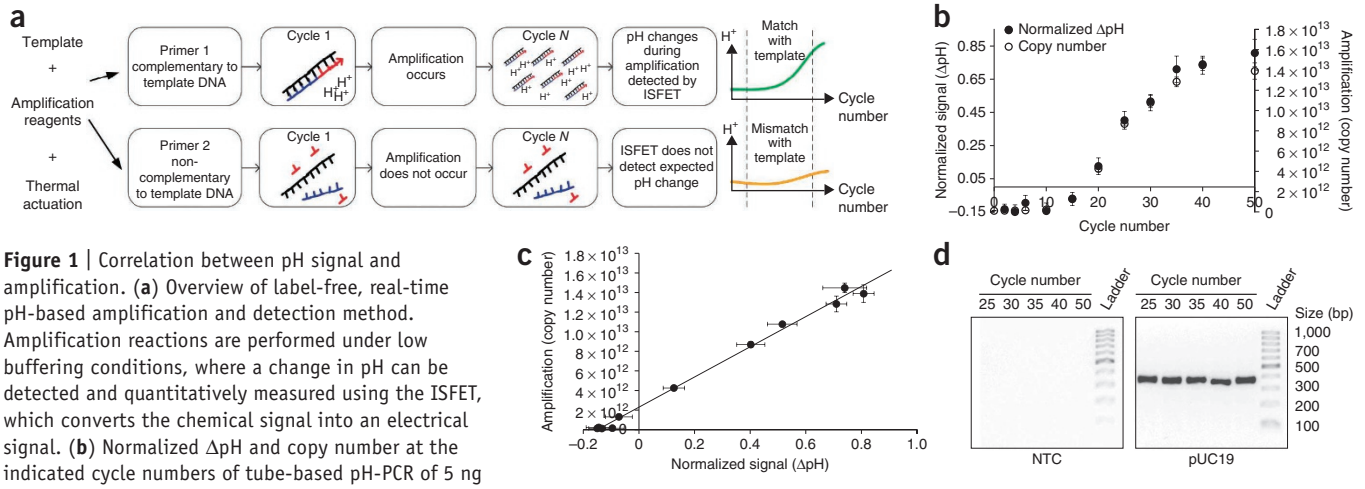

Figure 1 | Correlation between pH signal and amplification. (**a**) Overview of label-free, real-time pH-based amplification and detection method. Amplification reactions are performed under low buffering conditions, where a change in pH can be detected and quantitatively measured using the ISFET, which converts the chemical signal into an electrical signal. (**b**) Normalized ΔpH and copy number at the indicated cycle numbers of tube-based pH-PCR of 5 ng of pUC19. Error bars, s.d.; $n = 3$ experiments with each sample measured in triplicate. Normalized ΔpH was derived from subtracting the average pH of the no-template control reaction from the average pH of pUC19 reaction for the given cycle. (**c**) Correlation between average normalized ΔpH and total amount of accumulated double-stranded DNA by pH-PCR for the data in **b**. The solid black line is a linear regression fit ($R^2 = 0.994$) of the copy number. Error bars, s.d. (**d**) A representative gel for data as in **b**, showing the pH-PCR product from cycles 25–50.

to its target sequence initiates amplification. Successive incorporation of nucleotides leads to the liberation of hydrogen ions and consequently a decrease in pH of the reaction. The amplification does not proceed in reactions containing a mismatch primer, which do not result in a notable pH change (**Fig. 1a**).

We optimized the conditions for two established amplification techniques, PCR and LAMP, to perform amplification under low buffering conditions while retaining amplification efficiency and specificity. We termed these pH-sensitive amplifications pH-PCR and pH-LAMP to differentiate them from the conventional buffered methodologies.

As proof of principle, we addressed whether detecting a change in pH could be used as a reliable readout for amplification of nucleic acid. We performed pH-PCR in PCR tubes ('tube-based' reaction) to amplify a target sequence on pUC19 using a standard thermal cycler. To examine the temporal changes in pH, we terminated the reactions after various numbers of cycles and measured the pH using an ISFET-based pH probe. In parallel, we also measured the quantity of dsDNA. We observed a linear relationship, where the yield of DNA correlated with the magnitude of pH change, with an R^2 value of ~0.994 (**Fig. 1b**,**c**). The change in pH was unlikely due to nonspecific amplification as we only observed, by agarose gel electrophoresis, a single PCR product at the expected size (**Fig. 1d**). Similarly, for pH-LAMP reactions, we observed a strong correlation between the change in pH and amplification yield, with an R^2 value of 0.993 (**Supplementary Fig. 1**). In addition, the tube-based pH-PCR method can be used to reliably discriminate different SNP genotypes from purified genomic DNA and minimally prepared saliva samples (**Supplementary Fig. 2**). Together these data demonstrate specificity, robustness and reliability of using pH as readout for amplification.

An integrated circuit for DNA analysis

To create a system-on-chip for label-free analysis of nucleic acid, we designed an integrated circuit that can drive amplification and detection of nucleic acid in real time. The integrated circuit contains 40 ISFET sensors, 10 temperature sensors, resistive heating tracks, signal-processing circuitry and control circuitry all embedded in the chip, allowing continuous monitoring of pH (**Fig. 2** and **Supplementary Fig. 3**). The integrated circuit is fabricated using a standard CMOS fabrication process flow in commercial 0.35 µm CMOS production facilities used for production of computer and mobile phone chips[6,8,19,20].

This 4.8 mm × 5.5 mm integrated circuit comprises 120,000 transistors and is mounted on a disposable test card the size of a secure digital (SD) memory card (**Supplementary Fig. 4a**). The integrated circuit is controlled by a lightweight (20 g) analyzer board, which provides both power and a simple microcontroller interface to read digital data from the chip, sends control signals to the chip, performs genotyping and transfers results to an on-board display or personal computer (**Supplementary Fig. 4b–d**).

The integrated circuit has several important architectural design considerations that can be programmed to achieve desired functionality via the digital instruction block (**Fig. 2** and **Supplementary Fig. 3**). First, the on-chip processing and control circuitry, combined with on-chip heaters and temperature sensors, enables closed-loop temperature control. Combined with careful thermal design of the fluidic environment, the platform can perform thermal cycling or isothermal amplification, while continuously monitoring the reaction via the on-board ISFET sensors. Finally, there are on-chip analog-to-digital converters that convert raw sensor data to filtered digital information, which can be communicated off-chip using a standard serial peripheral interface bus. This on-chip digitization not only has advantages for enhancing signal-to-noise ratios and communication speeds, it also allows modularity through serial connection of multiple chips, which is a simple way to increase the number of ISFET sensors, thus increasing the number of reactions that can be interrogated at once. The on-chip digitization approach means that the number of connections (bondwires) exiting each chip can remain small, enabling the use of simple connectors such as the SD memory card format, which has just nine pins. As the architecture is scalable, the small number of connections to

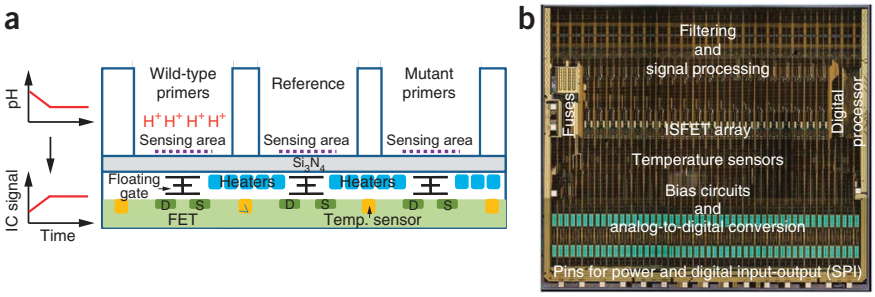

Figure 2 | Schematic representation of pH-sensing integrated circuit platform. (**a**) A simplified drawing of the cross-section of the array area showing ISFETs (floating gate, source (S) and drain (D)), temperature sensors (yellow squares) and digitally controlled resistive heater elements (blue squares) all embedded under the silicon nitride (Si_3N_4) sensing surface of the chip, all fabricated as part of the CMOS manufacturing process flow. The chip is beneath a polymer fluidic assembly or 'flow cell', which creates separate reaction chambers, each of which may contain a unique primer set. As exemplified in the chamber containing the wild-type primers, incorporation of nucleotides into the nascent nucleic acid strand results in proton production and a decrease in the pH of the reaction. The protons accumulate at the Si_3N_4 sensing surface resulting in an increase in the charge of the surface. This in turn increases the charge distribution in the channel (between source and drain) of the ISFET and increases the integrated circuit (IC) output signal voltage (IC signal) when the ISFET is biased at a fixed current. (**b**) CMOS-fabricated chip (right) showing key architectural modules.

peripheral electronics can be maintained even for very large ISFET arrays on a single chip.

On-chip real-time pH-sensitive amplification

To perform real-time amplification and detection on our pH-sensing semiconductor chip, we mounted three 2-µl chamber flow cells onto a chip connected to the electronic analyzer board where each chamber overlaps with one or more, typically two, ISFETs (**Fig. 2a**). This is done to introduce redundancy into the system and to decrease the alignment tolerances between the ISFETs and the reaction chambers within the fluidic assembly. One of the three reaction chambers functioned as a reference control chamber, which we used to cancel common-mode noise or non-ideal sensor behavior (electrochemical disturbances, sensor drift, temperature dependence and/or fabrication variability) that was not amplification-specific. We eliminated these effects by taking a differential measurement between ISFET signals derived from an experimental reaction (such as reactions containing primers matching the target sequence) and a reference control reaction (such as reactions lacking polymerase or a dNTP, or containing mismatching primers). As the reference control in this study, we used a reaction mixture lacking dTTP. We performed a no-template control reaction in a parallel chip to control for any nonspecific amplification (such as primer dimers).

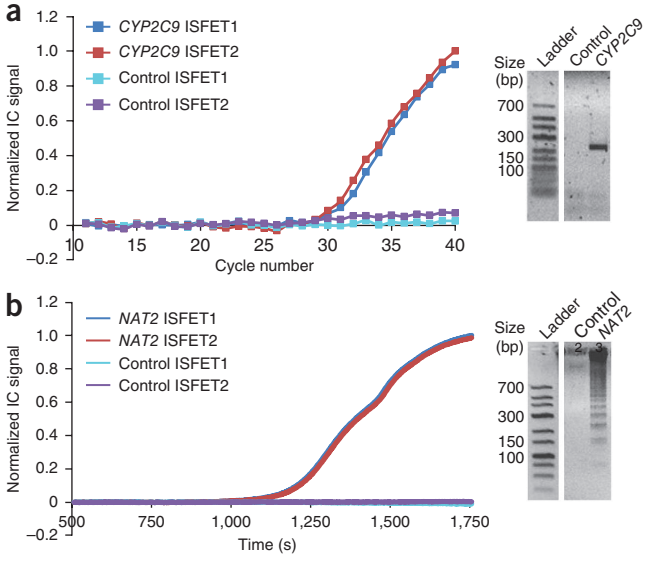

To experimentally establish the real-time performance as well as the thermocycling response of the integrated circuit assembly, we examined the ability of the integrated circuit to perform real-time PCR amplification (**Fig. 3a** and **Supplementary Figs. 5** and **6**). We dispensed pH-PCR amplification reagents containing primers targeting *CYP2C9*1* (430C)[21] and purified genomic DNA harboring homozygous wild-type alleles into two of the three chambers, and sealed the chambers with heat-resistant adhesive. The middle chamber was used as a reference control reaction. In parallel, no-template control reactions were performed in a separate chip. Using the embedded resistive heating module in the integrated circuit, we programmed the chip to perform a standard two-temperature PCR protocol (95 °C and 66 °C) and initiated real-time detection of pH signal. To make our system comparable to commercially available thermal cyclers used in the control experiments, we programmed the average ramp rate of the integrated circuit for heating and passive cooling to be at 3 °C s^{-1}. The amplification curves of the integrated circuit signal measured by changes in voltage were highly comparable to the fluorescence signals detected by the conventional real-time PCR apparatus (**Supplementary Fig. 5a**). Without any optimization of speed, a 40-cycle on-chip pH-PCR from purified human genomic DNA was completed in 35 min, and amplification was demonstrated by the progressive increase of differential voltage from cycle 30 (**Fig. 3a**). In addition, the progressive increase of the integrated circuit signal was proportional to product accumulation in the chamber (data not shown).

To ensure that the signal observed was not due to spurious amplification, we separated a fraction of each reaction mixture on an agarose gel and observed only one specific band in the amplification reactions, whereas we saw no observable bands in the no-template control reactions (**Fig. 3a**).

Figure 3 | On-chip amplification and detection using pH-PCR and pH-LAMP. (**a**) Representative on-chip pH-PCR amplification curves of homozygous wild-type *CYP2C9*1* allele. The control represents the no template reaction. The amplification curves represent the integrated circuit (IC) signal for the two ISFETs in a reaction chamber. Gels show product recovered from the chip at the end of the reaction (2% agarose gels; visualized by SYBR green). (**b**) Representative on-chip pH-LAMP amplification curves of *NAT2*. The control represents the no template reaction. The amplification curves represent the IC signal for the two ISFETs in a reaction chamber. Gels show products recovered from the chip at the end of the isothermal reaction, as in **a**.

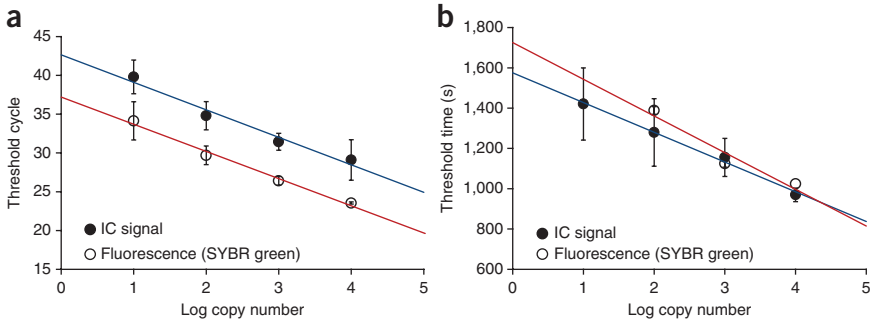

Figure 4 | Evaluation of integrated circuit sensitivity. (**a**) Standard curves of *GH1* gene generated from the on-chip pH-PCR and the conventional fluorescence-based SYBR green PCR. Mean ± s.d. of the threshold cycle (Ct) for the on-chip pH-PCR (two independent experiments, total of 6–8 chips per dilution) and SYBR green–based, tube-based PCR (two independent experiments, total of six replicates per dilution) were plotted against log of copy number of genomic DNA. The solid blue line is the linear regression fit (R^2 = 0.972) of the Ct values from the on-chip pH-PCR with a PCR efficiency (E) = 91.57%; the solid red line is the linear regression fit (R^2 = 0.990) of the Ct values from the conventional SYBR green PCR with E = 93.07%. $E = -1 + 10^{(-1/\text{slope})}$, where 'slope' is the slope of the linear regression fit. (**b**) Standard curves of *NAT2* gene generated from the on-chip pH-LAMP and the fluorescence-based SYBR green q-LAMP method. Mean ± s.d. of the threshold time for the on-chip pH-LAMP (5 independent experiments) and the fluorescence-based q-LAMP (2 independent experiments, six replicates per dilution) were plotted against log of copy number of genomic DNA. The solid blue line is the linear regression fit (R^2 = 0.993) of the threshold time from the on-chip pH-LAMP; the solid red line is the linear regression fit (R^2 = 0.937) of the threshold time from the fluorescence-based q-LAMP method.

We also evaluated the reproducibility of the integrated circuit platform by examining the intra- and inter-chip variability, and found that the coefficient of variation for the cycle threshold (Ct) of intra- and inter-chip data were low (**Supplementary Fig. 7** and **Supplementary Table 1**).

We next examined the performance of pH-LAMP on chip. We mixed primers targeting the N-acetyl transferase 2 gene (*NAT2*), which encodes an enzyme that helps metabolize drugs and other xenobiotics, with purified human genomic DNA. For the isothermal amplification, the integrated circuit was configured to heat and maintain the chip at a constant temperature while simultaneously monitoring the pH signal. We observed amplification of *NAT2* 1,200 s (20 min) after the start of the reaction but did not observe amplification in the control reaction (**Fig. 3b**).

To evaluate the sensitivity and the potential quantitative application of the integrated circuit platform, we performed on-chip pH-PCR of the human growth hormone 1 (*GH1*) gene over a tenfold serial dilution of haploid genome per chamber from purified human genomic DNA and compared the performance of the integrated circuit platform with the conventional SYBR green–based quantitative (q)PCR method (Applied Biosystems 'buffered' PCR mixture) using a fluorescence-based thermocycler (**Fig. 4a**). Both the integrated circuit and the optical platforms resulted in a comparable efficiency of PCR, 91.57% and 93.07%, respectively, and exhibited good linearity, whereby the correlation coefficient was 0.972 for the integrated circuit and 0.990 for the optical platform. Both the integrated circuit and the optical platforms consistently detected as few as 10 copies of genomic DNA (**Fig. 4a**).

Similarly, we performed pH-LAMP of the *NAT2* gene over a tenfold serial dilution of haploid genome per chamber of purified human K562 genomic DNA (**Fig. 4b** and **Supplementary Fig. 8**). Amplification over a range of serially diluted template exhibited good linearity (R^2 = 0.993) suggesting that our pH-based techniques are suitable for quantitative, real-time analysis of DNA. The lowest copy number that we consistently detected using the integrated circuit platform was 10 copies (signals detected in 19 of 20 reaction chambers). By comparison, tube-based q-LAMP performed on a standard thermocycling apparatus using the same minimum-buffered reaction conditions but with SYBR green as reaction indicator did not consistently amplify *NAT2* at 10 copies (**Fig. 4b**). The slope of both the SYBR green–based thermal cycler and pH-sensing integrated circuit system were comparable, suggesting that both platforms have similar thermal and detection performance.

Genotyping using a pH-sensing integrated circuit

To demonstrate potential clinical utility, we examined the ability of the platform to discriminate unique SNP variants of *CYP2C19* using pH-LAMP. We designed primer sets for amplification of the wild-type *CYP2C19* gene (*CYP2C19*1*) and two allelic variants, *CYP2C19*2* (81G>A) and *CYP2C19*17* (806C>T) that have opposing effects: *CYP2C19*2* is associated with poor metabolism of clopidogrel (Plavix) and *CYP2C19*17* is associated with ultrametabolism of the same drug[21]. We performed genotyping, where possible, from crude saliva extract. However, owing to a lack of *CYP2C19*2* mutant alleles in the collected saliva samples, we used commercially available purified human genomic DNA with the corresponding mutation for the experiment. We loaded the samples onto three-chamber flow cells mounted onto the chip, where one chamber contained primers targeting the wild-type allele *CYP2C19*1* (81G or 806C) and another chamber contained primers targeting one of the SNP variants, *CYP2C19*2* or *CYP2C19*17*. The middle chamber functioned as a reference control chamber containing primers to both wild type and mutants, but lacking dTTP. In this genotyping analysis, we used 30 samples (saliva and purified genomic DNA) for *CYP2C19*2* and 32 saliva samples for *CYP2C19*17* (**Supplementary Table 2**). We verified the genotypes of the saliva samples by the TaqMan genotyping assay. The integrated circuit data revealed that the pH-sensing integrated circuit platform correctly detected reactions with successful amplification in 29 of 30 samples for the *CYP2C19*2* analysis, and 30 of 32 samples for the *CYP2C19*17* analysis (**Supplementary Table 2**). We observed signal profiles of the possible combinations of diploid genotypes of *CYP2C19* alleles: the homozygous wild-type sample exhibited a notable change in voltage in reactions containing primers specific for the wild-type allele (*CYP2C19*1*), whereas the homozygous mutant sample exhibited a notable change in voltage in reactions containing primers specific to the mutant allele (*CYP2C19*2* or *CYP2C19*17*; **Fig. 5a,b**). For the heterozygous sample, reactions with primers specific to both the wild-type and mutant alleles exhibited amplification as indicated by a similar magnitude of voltage change.

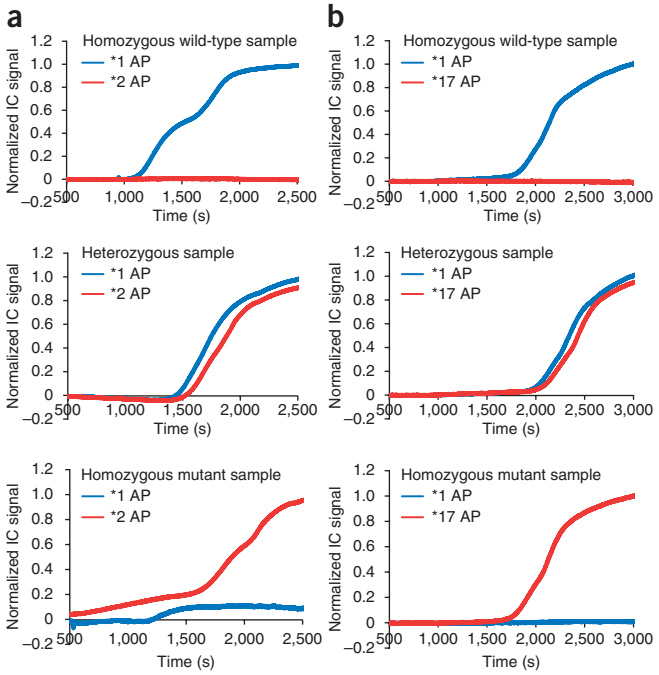

Figure 5 | SNP typing of *CYP2C19*2* and *CYP2C19*17*. (**a**,**b**) Integrated circuit (IC) pH-LAMP amplification and detection of *CYP2C19*1* and *CYP2C19*2* alleles (*1 and *2; **a**) and *CYP2C19*1* and *CYP2C19*17* alleles (*1 and *17; **b**) from crude human saliva samples. The amplification signals shown were normalized against control reference signal. AP, allele-specific primers.

Omission of genomic DNA template from the amplification reaction resulted in no amplification (data not shown). Similarly, we validated the genotype of wild-type and V600E mutation of BRAF, a proto-oncogene that encodes a serine/threonine protein kinase[22,23], using pH-LAMP on the integrated circuit platform (**Supplementary Fig. 9**).

To illustrate the scalability of our system, we designed a chip that contains four single chips serially connected (a quad chip). This allowed us to easily expand the capacity of the chip through more ISFETs and reaction chambers without redesigning the chip. To demonstrate the capability of the platform to multiplex multiple loci, we interrogated two known biomarkers of aging simultaneously using a 12-chamber flow cell mounted on a quad chip (**Supplementary Fig. 10**).

DISCUSSION

The scalability of the semiconductor platform, and the ability to quantitate, means that one can create chips with large sensor arrays to provide high-density, multiplexed molecular analysis platforms based on real-time detection of pH. The integrated circuit architecture with on-chip digitization enables it to daisy-chain and thus can be used in single-chip or multichip configurations onto which an application-specific flow cell and primer chemistry is mounted. We envision that with the appropriate fluidic interfaces, this semiconductor architecture can be used to transfer any current analytical techniques, including sequencing, microarrays and 'digital PCR'[24–31] into fast, integrated analysis platforms.

Overall, the amplification curves are comparable between fluorescence-based qPCR and on-chip pH-PCR. The integrated circuit for both PCR and LAMP reactions can detect as few as 10 genomic copies, which is comparable to other fluorescence-based microliter-scale lab-on-a-chip devices[32] and conventional fluorescence-based real-time qPCR instrumentation. We anticipate that with optimized reaction conditions, the sensitivity of both pH-PCR and pH-LAMP could be additionally enhanced.

The 25-µl fluorescence-based q-LAMP did not consistently detect 10 copies, whereas the fluorescence-based qPCR reliably detected 10 copies. We speculate that such discrepancy may be due to the difference in the concentration of SYBR green in the reaction mixture of fluorescence-based q-LAMP and qPCR. At present, we cannot exclude the possibly that with additional optimization of the fluorescence-based pH-LAMP reaction, we will be able to detect 10 copies.

The low intra- and interchip coefficients of variation observed (**Supplementary Fig. 7** and **Supplementary Table 1**) demonstrate a high reproducibility of the chip. The slight variability observed between different chambers may be due to pipetting errors as we loaded only 2 µl per chamber. The variability of the integrated circuit signals between chips can be higher than within a chip, which may be a result of minute differences in the assembly of the platform and temperature calibration (the platform is now assembled manually). Such differences may cause variations in the sealing of the chamber or temperature variations. Such technical variability can be minimized by integrating seamless sample preparation and delivery to the chip as well as automated rather than manual assembly of the platform.

Although here we used a 2-µl reaction volume, with additional optimization of the microfluidics, the reaction volume can be decreased. It has been shown that decreasing the reaction volume has clear advantages such as greater sensitivity[31,32], less contamination[27], lower cost and greater throughput[27], and thus is important in the development of a portable and scalable platform for amplification and detection of nucleic acid.

The size of the chambers as well as the chip and sensors are scalable and can be designed and fabricated depending on the number of samples or genetic markers to be interrogated at once. For example, we performed allele-specific probe-extension assays using a five-chamber flow cell on a single chip integrated circuit platform to simultaneously genotype two alleles (**Supplementary Fig. 11** and **Supplementary Table 3**). In addition, without redesigning the architecture of the chip, we increased the number of sensors and chambers, and demonstrated the capability to multiplex by daisy-chained four single chips (**Supplementary Fig. 10**). Evidently, a single chip can also be designed to contain millions of sensors and wells[15]. Together, these illustrate the flexibility of the semiconductor-based platform.

The integrated circuit platform lends itself to amplification strategies other than PCR and LAMP as long as (i) hydrogen ions can be monitored as a readout for amplification of nucleic acid, (ii) the reaction can be performed under low buffering capacity and (iii) enzyme activity can be maintained over a favorable range of pH.

The technology opens the door for development of a portable, point-of-care platform for analyzing nucleic acids, which can move personalized medicine to the clinic and overcome issues such as turnaround time associated with laboratory-based tests.

METHODS

Methods and any associated references are available in the online version of the paper.

Note: Supplementary information is available in the online version of the paper.

ACKNOWLEDGMENTS

We thank T.S.K.T. Lim for his support and vision in semiconductor-based DNA analysis, T. Cass for his guidance and expert opinion, and the entire DNA Electronics team for their contributions to our wider work.

AUTHOR CONTRIBUTIONS

C.T. invented the technology and supervised the project with S.C.R. and L.M.S.; D.M.G., H.B., B.C., P.G. and J.C.J. designed the chips and electronics; A.P., P.A. and D.C.-A. designed the integrated test card, fluidics and electrochemistry; C.-P.O., C.-J.A.W., M.L.M., L.Z., A.P. and G.I.C. designed the molecular biological methods and assays; G.I.C., K.A.-D., K.S.J., R.E.T., D.C.-A., D.M., S.S., S.T. and I.M.Q.B. performed the research; G.I.C., L.M.S., S.C.R., C.-P.O., C.-J.A.W. and P.G. wrote the manuscript.

COMPETING FINANCIAL INTERESTS

The authors declare competing financial interests: details are available in the online version of the paper.

1. Holland, P.M., Abramson, R.D., Watson, R. & Gelfand, D.H. Detection of specific polymerase chain reaction product by utilizing the 5′-3′ exonuclease activity of *Thermus aquaticus* DNA polymerase. *Proc. Natl. Acad. Sci. USA* **88**, 7276–7280 (1991).
2. Higuchi, R., Fockler, C., Dollinger, G. & Watson, R. Kinetic PCR analysis: real-time monitoring of DNA amplification reactions. *Nat. Biotechnol.* **11**, 1026–1030 (1993).
3. Heid, C.A., Stevens, J., Livak, K.J. & Williams, P.M. Real-time quantitative PCR. *Genome Res.* **6**, 986–994 (1996).
4. Wittwer, C.T., Herrmann, M.G., Moss, A.A. & Rasmussen, R.P. Continuous fluorescence monitoring of rapid cycle DNA amplification. *Biotechniques* **22**, 130 (1997).
5. Toumazou, C. & Purushothaman, S. Sensing apparatus and method. US patent 7,686,929 (2002).
6. Toumazou, C., Purushothaman, S. & Ou, C.-P. qPCR using solid-state sensing. US patent 7,888,015 (2007).
7. Bousse, L., De Rooij, N.F. & Bergveld, P. Operation of chemically sensitive field-effect sensors as a function of the insulator-electrolyte interface. *IEEE Trans. Electron. Dev.* **30**, 1263–1270 (1983).
8. Bausells, J., Carrabina, J., Errachid, A. & Merlos, A. Ion-sensitive field-effect transistors fabricated in a commercial CMOS technology. *Sens. Actuators B Chem.* **57**, 56–62 (1999).
9. Jakobson, C.G., Dinnar, U., Feinsod, M. & Nemirovsky, Y. Ion-sensitive field-effect transistors in standard CMOS fabricated by post processing. *IEEE Sens. J.* **2**, 279–287 (2002).
10. Bergveld, P., DeRooij, N.F. & Zeme, J.N. Physical mechanisms for chemically sensitive semiconductor devices. *Nature* **273**, 438–443 (1978).
11. Bergveld, P. ISFET, theory and practice. *IEEE Sens. Conf. Toronto* 1–26 (IEEE, 2003).
12. Purushothaman, S., Toumazou, C. & Georgiou, J. Towards fast solid state DNA sequencing. *IEEE Int. Symp. on Circuits and Systems* 169–172 (IEEE, 2002).
13. Purushothaman, S., Toumazou, C. & Ou, C.-P. Protons and single nucleotide polymorphism detection: a simple use for the Ion Sensitive Field Effect Transistor. *Sens. Actuators B Chem.* **114**, 964–968 (2006).
14. Garner, D.M. *et al.* A multichannel DNA SoC for rapid point-of-care gene detection. *IEEE International Solid-State Circuits Conference* **57**, 492–493 (2010).
15. Rothberg, J.M. *et al.* An integrated semiconductor device enabling non-optical genome sequencing. *Nature* **475**, 348–352 (2011).
16. Thewes, R. *et al.* Sensor arrays for fully-electronic DNA detection on CMOS. *IEEE International Solid-State Circuits Conference. Digest of Technical Papers* 350–473 (2002).
17. Pourmand, N. *et al.* Direct electrical detection of DNA synthesis. *Proc. Natl. Acad. Sci. USA* **103**, 6466–6470 (2006).
18. Notomi, T. *et al.* Loop-mediated isothermal amplification of DNA. *Nucleic Acids Res.* **28**, E63 (2000).
19. Matsuo, T. & Esashi, M. Methods of isfet fabrication. *Sens. Actuators* **1**, 77–96 (1981).
20. Errachid, A., Zine, N., Samitier, J. & Bausells, J. FET-based chemical sensor systems fabricated with standard technologies. *Electroanalysis* **16**, 1843–1851 (2004).
21. Hiratsuka, M. *In vitro* assessment of the allelic variants of cytochrome P450. *Drug Metab. Pharmacokinet.* **27**, 68–84 (2012).
22. Tsao, H., Chin, L., Garraway, L.A. & Fisher, D.E. Melanoma: from mutations to medicine. *Genes Dev.* **26**, 1131–1155 (2012).
23. Benlloch, S. *et al.* Detection of BRAF V600E mutation in colorectal cancer: comparison of automatic sequencing and real-time chemistry methodology. *J. Mol. Diagn.* **8**, 540–543 (2006).
24. Niemz, A., Ferguson, T.M. & Boyle, D.S. Point-of-care nucleic acid testing for infectious diseases. *Trends Biotechnol.* **29**, 240–250 (2011).
25. Yeung, S.S.W., Lee, T.M.H. & Hsing, I.-M. Electrochemistry-based real-time PCR on a microchip. *Anal. Chem.* **80**, 363–368 (2008).
26. Deféver, T. *et al.* Real-time electrochemical monitoring of the polymerase chain reaction by mediated redox catalysis. *J. Am. Chem. Soc.* **131**, 11433–11441 (2009).
27. Burns, M. An integrated nanoliter DNA analysis device. *Science* **282**, 484–487 (1998).
28. Neuzil, P., Pipper, J. & Hsieh, T.M. Disposable real-time microPCR device: lab-on-a-chip at a low cost. *Mol. Biosyst.* **2**, 292–298 (2006).
29. Ottesen, E.A., Hong, J.W., Quake, S.R. & Leadbetter, J.R. Microfluidic digital PCR enables multigene analysis of individual environmental bacteria. *Science* **314**, 1464–1467 (2006).
30. Wong, H.S. & White, M.H. A self-contained CMOS integrated pH sensor. *International. Electron Devices Meeting, Technical Digest* 658–661 (1988).
31. Heyries, K.A. *et al.* Megapixel digital PCR. *Nat. Methods* **8**, 649–651 (2011).
32. Stedtfeld, R.D. *et al.* Gene-Z: a device for point of care genetic testing using a smartphone. *Lab Chip* **12**, 1454–1462 (2012).

ONLINE METHODS

Primers and human genomic DNA and saliva samples. All primers were synthesized by ThermoFisher or Integrated DNA Technology (IDT) and are listed in the **Supplementary Table 4**.

Purified human genomic DNA used in the present study were obtained from Coriell Institute for Medical Research and are listed in **Supplementary Table 5**.

Informed consent was obtained from all saliva donors. Approval was received from NHS Research Ethics Committee London (REC Reference 08/H0706/2).

pH-sensitive amplification in test tubes. pH-PCR experiments were performed in a 35 µl reaction volume. The reaction mixture consisted of 50 mM KCl, 3 mM $MgCl_2$, 0.5 mM dNTPs, 1 mg/ml BSA, 1 µM of forward and reverse primers each, 0.8 M betaine, 0.1% Triton-X 100 and 0.3 µl of hot-start Taq DNA polymerase. The pH of the reaction mixture was adjusted to 8–8.5 before the addition of 1 ng of pUC19 plasmid DNA, 10 ng of purified genomic DNA, ~3,000 copies of *CYP2C9*2* plasmid DNA or 1–3.5 µl of crude saliva lysates (equivalent to approximately 10 ng or 3,000 copies of genomic DNA). Control reaction without template was set up in parallel. The thermocycling program for pUC19 pH-PCR was set up as follows: 95 °C for 2 min followed by 50 cycles of 95 °C for 15 s and 70 °C for 15 s (Piko Finnzymes, ThermoFisher). The thermocycling program for *CYP2C9*1* and *CYP2C9*2* was set up as follows: 95 °C for 1 min followed by 40 cycles of 95 °C for 10 s and 66 °C for 15 s. pH measurements were conducted before and after thermocycling using ISFET-based pH probe (Sentron). Amplification yield was quantified using Qubit & Quant-iT HS kit (Life Technologies) per the manufacturer's instructions.

pH-LAMP experiments were performed in a 35-µl reaction volume. The reaction mixture consisted of 50 mM KCl, 5 mM $MgSO_4$, 5 mM NH_4Cl, 1 M betaine (Sigma Aldrich), 1 mg/ml BSA, 0.1% Triton-X 100, 2.8 mM dNTP, 1.6 µM each of forward inner primer (FIP) and backward inner primer (BIP), 0.8 µM each of loop-forward (Loop-F) and loop-backward (Loop-B) primers, 0.2 µM each of forward outer primer (F3) and backward outer primer (B3) and Bst polymerase (New England Biolabs). The pH of the reaction mixture was adjusted to between pH 8.5 and 8.8 before addition of 10 ng or indicated copy number of purified human genomic DNA (Coriell Institute for medical Research). Control reaction without template was set up in parallel. The reactions were performed at 63 °C; pH and amplification yield were determined as described for pH-PCR.

Time-course experiments were performed by terminating the reactions at different cycle number (pH-PCR) or time (pH-LAMP), and both pH and amplification yield were quantified using ISFET-based pH probe (Sentron) and Qubit (Life Technologies), respectively.

On-chip real-time pH-PCR and pH-LAMP. The preparation for on-chip real-time pH-PCR was performed essentially as described for the tube-based assay. Routinely, 10 ng of human genomic DNA were added to the 35-µl pH-PCR mixture. After preparation of the reaction mixture, 2 µl of the 35-µl reaction mixture were dispensed into a reaction chamber mounted on the integrated circuit, which was fitted onto an SD memory card, and sealed with a heat-resistant adhesive. For a three-chamber flow cell, one of the chambers was used as a reference chamber that contained a mixture of primers targeting the wild-type and mutant alleles, and template, but lacked the nucleotide dTTP. The SD memory card (with integrated circuit) was then connected to an analyzer board, and the integrated circuit was activated to perform the thermocycling program of an initial 95 °C denaturation for 2 min, followed by 40 cycles of 95 °C for 15 s and 66 °C for 17 s for *CYP2C9*. The on-chip pH-PCR for *GH1* gene was performed under the following conditions: initial activation at 95 °C for 2 min, followed by 50 cycles of 95 °C for 20 s and 64 °C for 30 s. On-chip pH-PCR for pUC19 was performed under the following conditions: initial activation at 95 °C for 2 min, followed by 50 cycles of 95 °C for 15 s and 70 °C for 17 s.

The preparation for on-chip real-time pH-LAMP was performed essentially as described for the tube-based assay. Routinely, 1–10ng of human genomic DNA or 1–3.5 µl of crude saliva lysates were added to the 35-µl pH-LAMP reaction mixture. The crude saliva lysates were prepared by mixing saliva with lysis buffer (25 mM NaOH and 200 µM EDTA) in a 3:5 saliva:lysis buffer ratio. After preparation of the reaction mixture, 2 µl of the 35 µl reaction mixture were dispensed into the chamber mounted on the integrated circuit. The reference chamber was set according to the method described for on-chip pH-PCR. The on-chip LAMP reactions were performed at constant 63 °C for *NAT2* and 63 °C for allele-specific pH-LAMP (*CYP2C19*2*, *CYP2C19*17*, *MMP1*, *NQO1*, *BRAF* wild type and *BRAF V600E*), and terminated at appropriate time for each experiment. For both pH-PCR and pH-LAMP, after termination of the reactions, DNA was retrieved from each reaction chamber, and quantified and analyzed by Qubit (Life Technologies) and separated on 2% agarose gel, respectively.

pH-PCR with various genomic DNA templates. Purified human genomic DNA was used in this study, where starting copy number varied from 0, 1, 10, 100, 1,000 and 10,000 copies per 2 µl chamber. The on-chip pH-PCR for *GH1* gene were performed under the following conditions: initial activation at 95 °C for 2 min, followed by 50 cycles of 95 °C for 20 s and 64 °C for 30 s. On each chip, two chambers containing the same PCR fluid served as analytical replicates, and the third chamber was used as a reference, which lacked the dTTP nucleotide. Average Ct and s.d. from all chips included in this study for each copy number were plotted against log copy number. Error bars represent the variation (s.d.) between chips and between chambers.

For the conventional SYBR green PCR method, the indicated copy number of human genomic DNA (0, 1, 10, 100, 1,000, 10,000 copies) was added to the 35-µl SYBR-green PCR Master Mix (Applied Biosystems, Life Technology) containing 1 µM each of *GH1* forward and reverse primer. The PCRs were performed under the following conditions using the ep Mastercycler RealPlex (Eppendorf): initial activation at 95 °C for 10 min, followed by 50 cycles of denaturation at 95 °C for 20 s and annealing and denaturation at 64 °C for 30 s.

For both pH-LAMP and pH-PCR, the threshold time and cycle were determined by identifying the log-linear range using a logarithmic amplification plot. The threshold line was adjusted to a value just above the baseline of an amplification curve (nonlogarithmic) but situated in the log-linear range.

pH-LAMP with various genomic DNA templates. Purified human genomic DNA from K562 cells was used in this study, where starting copy number varied from 1, 10,100, 1,000, and 10,000 copies per 2-µl chamber. The on-chip LAMP reactions were performed at

constant 63 °C for *NAT2*. In each pH-LAMP run, ten integrated circuit chips were used to address five copy number variations (two chips each for no-template control, 10, 100, 1,000, 10,000 copies). On each chip, two chambers containing the same LAMP fluid serves as experimental duplicates, with the other chamber lacking dTTP as reference. The 10-chip run was repeated five times. Absolute mean time to detection (equivalent to Ct) was plotted against log target copy number. Error bars represent the variation (s.d.) between chips and between chambers.

For SYBR-green detection method, indicated copy number of human genomic DNA were added to the 25-µl reaction mixture containing 50 mM KCl, 5 mM $MgSO_4$, 5 mM NH_4Cl, 1 M Betaine (Sigma Aldrich), 1 mg/ml BSA, 0.1% Triton-X 100, 2.8 mM dNTP, 1.6 µM each of FIP and BIP primers, 0.8 µM each of Loop-F and Loop-B primers, 0.2 µM each of F3 and B3 primers, Bst polymerase (New England Biolabs), and 0.25 µl of SYBR Green I (Life Technologies) . The q-LAMP reactions were performed at a constant 63 °C for *NAT2* using ep Mastercycler RealPlex (Eppendorf).

Reproducibility of the integrated circuit platform. Intra- and inter-chip variability were determined in three independent experiments, where each experiment consists of a set of chips, and all the chambers for all the chips (two chambers per chip, excluding reference chamber) were dispensed with same pH-PCR reagent targeting either *GH1* or *CYP2C9*1* (**Supplementary Fig. 7** and **Supplementary Table 1**). The amplification was monitored in real time using the integrated circuit platform.

Integrated circuit design and fabrication. The integrated circuit for the architecture shown in **Supplementary Figure 2** was designed and simulated using the Cadence Virtuoso Schematic Editor (Cadence) and then the physical chip layout was performed in Cadence Virtuoso Layout Editor (Cadence) to create a graphic database system (GDS) file. This file was then sent to a foundry where the integrated circuits were fabricated using standard unmodified CMOS 0.35 µm process on 200-mm wafers, and subsequently diced into individual chips of 26.34 mm^2. As the integrated circuit can perform on-chip DNA amplification using its integrated heaters, sensor performance does not require optimization, thus a silicon nitride (Si_3N_4) insulating layer can be used as the sensing layer, which is part of the standard CMOS fabrication process.

The integrated circuit contained forty ISFET sensors, ten temperature sensors, resistive heating tracks, signal processing and control circuitry all embedded within the chip. The 4.8 mm × 5.5 mm integrated circuit comprised 120,000 transistors and was mounted on a disposable test card the size of an SD memory card.

Each 104 µm × 34 µm ISFET sensor on the integrated circuit contained an electrically floating gate, which is a consequence of the CMOS manufacturing process where there will always be a polysilicon gate on top of the gate oxide of the transistor[19]. For chemistries requiring greater sensitivity, the sensing layer of the integrated circuit can be replaced by thin high-dielectric metal oxide using extra mask steps in the CMOS fabrication process[9,15,19] (**Supplementary Note 1**). Note that the ISFET has an output signal proportional to pH in the solution to which its ion-sensitive insulating layer is exposed and that ΔpH will be dependent on the amount of nucleotide incorporation during synthesis of nucleic acid (**Supplementary Note 1**).

Temperature control was provided by driving the on-chip resistive heater via a class A heater driver circuit, and then using an external proportional-integral-derivative (PID) control algorithm to set the temperature of the chip within ± 0.1 °C, which was monitored by the on-chip diode-based temperature sensors, with a size of 84 µm × 84 µm.

The integrated circuit was then wirebonded and encapsulated onto a PCB substrate with a SD card format. The sensing area of chip was left exposed, which allowed a polymer flow cell to be vertically mounted and bonded to create individual chambers. The flow cell provided access ports for sample introduction and reaction chambers to isolate separate reaction volumes for unique amplification reactions to take place within them (**Fig. 2**). The integrated circuit was powered and controlled by a lightweight (20 g) analyzer board, which provided both power and a simple microcontroller interface to read digital data from the chip, sent control signals to the chip, performed genotype or sequence calling, and transferred results to an on-board display or PC (**Supplementary Fig. 4b**).

Data analysis. Integrated circuit signals for pH-PCR and pH-LAMP were collected continuously with the sampling rate set at 16 Hz (16 data points per second). During data processing, the raw data obtained for pH-PCR and pH-LAMP were down-sampled to one data point per cycle and one data point per second (1 Hz), respectively. Drift correction was performed by curve-fitting the data from each ISFET using data points from the first few minutes or cycles of the amplification reaction; because of the low DNA copy number at the early stage of the reaction, the integrated circuit signal is dominated by sensor drift rather than by amplification-specific pH signal.

To remove common-mode effects, ISFET signals (in millivolts (mV)) from the reference chamber were subtracted from ISFET signals derived from the experimental chambers (ΔmV). The curves were normalized by dividing each ΔmV value by the maximum ΔmV value, and plotted against time or cycle.

Allele-specific probe extension. Single-stranded DNA with the target SNP in the sequence was amplified by PCR, digested and purified using Qiagen PCR Cleanup kit (Qiagen). Purified single-stranded DNA was subjected to an additional buffer exchange step to remove excessive Tris buffer in the sample. A five-chamber flow cell was mounted onto the integrated circuit to accommodate all four allele-specific probes (*CYP2C9*2* wild type and mutant, and *CYP2C9*3* wild type and mutant). Single-stranded DNA at a final concentration of 5 µM was mixed with 7.5 µM of each of the allele-specific DNA probe with the allele placed on the 3′ end, twofold excess of dNTPs, 50 mM KCl and 5 mM $MgCl_2$. Integrated circuit with five-chamber flow cell was stabilized with non-DNA buffer in all five chambers during the mixing and preparation.

Before injecting into each of the reaction chambers in the flow cell, the DNA mixture with each of the allele-specific primers was mixed with Bst enzyme on ice at a final concentration of 0.25 U/µl. The chilled reaction mixture was then injected into the chamber, displacing the non-DNA buffer instantly for immediate signal recording. One chamber would remain stabilized with the original non-DNA buffer as baseline. After injecting all four allele variants, the integrated circuit signal from each corresponding sensor was recorded and analyzed for determination of genotype.

doi:10.1038/nmeth.2520